Biomaterials Science

ROYAL SOCIETY OF CHEMISTRY

PAPER

View Article Online
View Journal | View Issue

Cite this: *Biomater. Sci.*, 2020, **8**, 2921

Bacterial nanocellulose as a corneal bandage material: a comparison with amniotic membrane†

Irene Anton-Sales, [a] Justin Christopher D'Antin, [b,c] Jorge Fernández-Engroba, [b,c] Victor Charoenrook, [b,c] Anna Laromaine, *[a] Anna Roig *[a] and Ralph Michael [b,c]

Corneal trauma and ulcerations are leading causes of corneal blindness around the world. These lesions require attentive medical monitoring since improper healing or infection has serious consequences in vision and quality of life. Amniotic membrane grafts represent the common solution to treat severe corneal wounds. However, amniotic membrane's availability remains limited by the dependency on donor tissues, its high price and short shelf life. Consequently, there is an active quest for biomaterials to treat injured corneal tissues. Nanocellulose synthetized by bacteria (BNC) is an emergent biopolymer with vast clinical potential for skin tissue regeneration. BNC also exhibits appealing characteristics to act as an alternative corneal bandage such as; high liquid holding capacity, biocompatibility, flexibility, natural – but animal free-origin and a myriad of functionalization opportunities. Here, we present an initial study aiming at testing the suitability of BNC as corneal bandage regarding preclinical requirements and using amniotic membrane as a benchmark. Bacterial nanocellulose exhibits higher mechanical resistance to sutures and slightly longer stability under *in vitro* and *ex vivo* simulated physiological conditions than amniotic membrane. Additionally, bacterial nanocellulose offers good conformability to the shape of the eye globe and easy manipulation in medical settings. These excellent attributes accompanied by the facts that bacterial nanocellulose is stable at room temperature for long periods, can be heat-sterilized and is easy to produce, reinforce the potential of bacterial nanocellulose as a more accessible ocular surface bandage.

Received 15th January 2020,
Accepted 3rd April 2020

DOI: 10.1039/d0bm00083c

rsc.li/biomaterials-science

Introduction

Ocular surface disorders, especially those affecting the cornea, can severely disturb vision and quality of life. Yearly, there are approximately 1.5 million worldwide cases of corneal trauma, burns and infectious ulcerations.[1,2] Conjunctival flap operations have long been performed in these cases,[3–5] but due to its poor post-operative visual and cosmetic results, during the last decades, human amniotic membrane (AM) patches[6–8] have been preferred because of their well-known regenerative effects.[9] The AM has a layered structure with two well differentiated sides: an epithelial side made of cuboidal cells and a spongy stromal side constituted mainly of collagen fibres[10] which is typically placed in contact with the corneal damage. AM also offers a tectonic pillar for corneal perforations and can be indicated as a temporary treatment prior to a reconstructive technique.[11] Despite its satisfactory clinical outcomes,[12,13] AM sometimes degrades faster than the required healing time,[14] it is extremely costly and it has a short shelf life. Other drawbacks of AM concern its availability, which depends on donors and the presence of tissue banks and medical infrastructure. Therefore, novel biomaterials able to overcome these limitations are currently being investigated.[15–17]

Bacterial nanocellulose (BNC) is a polysaccharide naturally secreted by several non-pathogenic bacterial strains that has gained a lot of attention for biomedical applications.[18,19] BNC can easily be produced from *Komagataeibacter xylinus* (*K. xylinus*) cultures as stable water-insoluble hydrogels at the interface between the air and the liquid culture medium. After appropriate cleaning, BNC hydrogels are free of endotoxins and ultra-pure, containing just nanocellulose fibres organized in a similar structure as collagen.[20] Furthermore, BNC exhibits a high liquid holding capacity, porosity and conformability together with numerous functionalization opportunities due to its high surface area. All these unique characteristics promote the many valuable applications of BNC as a biomaterial. In fact, BNC has successfully been used for skin tissue

[a]*Institute of Materials Science of Barcelona (ICMAB-CSIC), Spain. E-mail: alaromaine@icmab.es, anna.roig@csic.es*
[b]*Institut Universitari Barraquer, Universitat Autònoma de Barcelona, Barcelona, Spain*
[c]*Centro de Oftalmología Barraquer, Barcelona, Spain*

†Electronic supplementary information (ESI) available. See DOI: 10.1039/d0bm00083c

regeneration[21–23] and products like Epicite[hydro] (JenaCell) are already available on the market. Similarly, a BNC-based coating for implantable devices (Hylomate Pouch[24]) is in the final stages of validation as an anti-fibrotic agent. Other studies highlight the potential of BNC as substrate for *in vitro* models[25] and as a drug delivery matrix.[26,27]

Despite these promising reports, the capability of BNC to heal other body surfaces such as the cornea or the dura mater[28] remain largely unexploited.[29] Therefore, based on the outstanding performance of BNC on skin wound healing, we hypothesize that BNC also holds potential as an ocular surface bandage. In contrast to AM, BNC is stable at room temperature for long periods of time and its production from diverse carbon sources is sustainable and controllable in terms of size, shape and thickness.[30] Finally, yet importantly, BNC can be easily sterilized by heat and its animal-free origin might reduce the risk of disease transmission, ethical concerns and dependency on donor tissues. BNC's light transmittance is around 70% due to light scattering caused by fibre bundles and pores.[31] Since this might limit its applicability as a long-term corneal substitute, we focused on a temporal application of BNC similar to that of AM.[32]

Here, we validate BNC as suitable base material to develop novel corneal bandages. A detailed comparison between physicochemical characteristics of AM and BNC is provided and then, we demonstrate BNC's mechanical resistance to suture and stability under physiological conditions. Finally, we show preliminary *ex vivo* assays with porcine corneas. Together our results endorse BNC as a strong candidate for future corneal bandaging applications.

Results

Material characterization

Despite the extensive use of AM in ophthalmology, not much has been reported about its micro/nanostructure and material characteristics. Consequently, prior to the stability tests, the main characteristics of BNC and AM were compared. Scanning electron microscopy (SEM) was employed to study the micro and nanostructures of the ocular surface bandages. SEM imaging (Fig. 1A) of AM revealed a distinct micro and nanostructure of its two sides. The stromal side, which is generally placed in contact to the corneal surface, exhibits a nanofibrillar structure that highly resembles the BNC's architecture. The mean fibre diameter measured from the SEM images was 57 ± 9 nm for the collagen fibres in AM and 56 ± 13 nm for BNC nanofibers (average value from both sides of BNC). The epithelial side of AM is more unorganized and fibres were not observed. BNC presented a rather similar structure at both sides. However, the top side oriented towards the air during the biosynthesis process shows higher compaction of the fibres than the side facing the liquid bacterial culture (Fig. 1A).

BNC hydrogels were investigated as-synthetized, containing high amounts of water (≈100 times its own dry weight). A dehydration test revealed that BNC hydrogels exposed to the air under controlled temperature (22 °C) and humidity (45%) still maintain two thirds of their initial water content after 6 hours (see ESI Fig. S1†). AM membranes were also used as-received from the tissue bank. Thicknesses measured with a micrometer were between 600 and 900 μm for BNC, while AM pieces were much thinner (between 50 and 110 μm). These

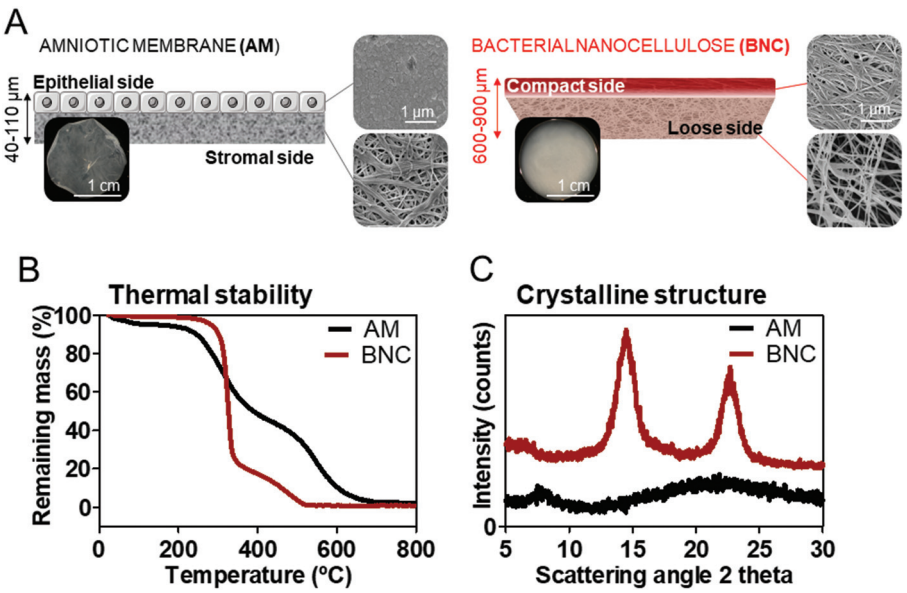

Fig. 1 Materials characterization. (A) Micro and nano structure of the bandage materials tested. Each material presents two differentiated sides, which are illustrated schematically and with SEM micrographs. The stromal side of AM and the compact side of BNC were the ones facing the ocular tissues in the experiments detailed below. (B) Representative TGA curves of BNC and AM (n = 3 for each material). Remaining mass of BNC is 0.7 ± 0.1% and AM is 1.7 ± 0.8%. (C) X-ray diffraction patterns of the ocular surface bandages where BNC shows two broad diffraction peaks while AM appears as an amorphous material.

thickness measurements can be slightly affected by the blotting performed prior to the measurement to remove the excess water of the films and therefore the superficial mass parameter was monitored instead of the thickness on the onward experiments. BNC superficial mass computed was almost 8 times higher than AM (90 *vs.* 12 mg cm^{-2}).

Regarding optical properties, both materials exhibit low visible light absorbance (<1 absorbance from 800 to 400 nm) displaying a progressive increase in light absorbance towards the ultraviolet range. Interestingly, despite the marked difference in thickness, the overall ultraviolet-visible light absorbance was not proportionally higher in BNC. As an example, light absorbance for BNC was 0.38 at 600 nm and 0.29 for AM.

The thermal stability of the materials was assessed by thermo-gravimetric analysis (TGA) (Fig. 1B). The onset of degradation was defined by the position of the peaks from the first derivative function of the TGA curves and happened at ≈325 °C for BNC and at ≈250 °C for AM. Both materials decomposed almost completely (BNC total degradation happened at approx. 500 °C and AM at approx. 650 °C) and show residual masses of 0.7 ± 0.1% for BNC and 1.7 ± 0.8% for AM (n = 3). This result indicates that both materials are almost entirely constituted by organic matter as expected.

To gain insight into the atomic organization of BNC and AM, their X-Ray diffraction (XRD) patterns were compared (Fig. 1C). BNC is a semi-crystalline material that presents two characteristic broad diffraction peaks (at 2θ = 14.6 and 22.8) as well as some amorphous background.[33] Contrarily, AM does not show any clear diffraction pattern, indicating an amorphous structure.

Suture stress test

An important specification of an ocular surface bandage material is to enable an easy and durable suturing to the eye surface. Since AM is commonly sutured in ophthalmological procedures, it was used as a benchmark for comparison. BNC has been satisfactorily sutured *in vivo*[34] but, to the best of our knowledge, not to the ocular tissues and its resistance to suture has never been quantified. A set up was assembled similar to the one reported in ref. 35 and illustrated in Fig. 2A. BNC and AM samples were sutured to small pieces of scleral tissues and clamped. Weights were added until BNC and AM materials teared at the suture point as shown in Fig. 2B. BNC films held an average force of 0.47 ± 0.11 N while AM resistance was much lower (0.11 ± 0.02 N). Some of the BNC pieces tolerated higher loads and caused the suture thread to break before BNC (filled dots on the graphs in Fig. 2B). Statistical analysis (unpaired T-test) revealed a significant difference between the two maximum forces supported by the compared materials.

Stability under simulated physiological conditions

Another requisite to consider a material for ocular bandaging applications is its durability and stability under the eye's physiological conditions. To gain insight on BNC's bio-stability we performed *in vitro* and *ex vivo* tests. For these tests, native BNC hydrogels were used since dry films have a paper-like appearance that showed poorer conformability to the dome shape of the eye globes. For the *in vitro* study, BNC and AM were maintained in corneal preservation medium to monitor its potential degradation. The integrity of the samples was inferred by measuring their superficial mass and by visual observation. No indications of degradation were noticed for any of the two materials as depicted in Fig. 3. The materials did not show any substantial change in diameter or thickness (see slit lamp pictures). In addition, no disintegration features or holes were observed in any of the samples. Visually, AM samples became more opaque after the 30-day incubation while BNC samples maintained their transparency but acquired some shading from the culture medium. These visual observations were confirmed by measuring the grey values of the dark field images taken for each sample before and after incubation (dark field pictures are shown in Fig. S2†). The grey values of AM samples considerably increased upon incubation (from 77 ± 7 to 162 ± 7) while similar grey values for BNC were conserved after the incubation period (79 ± 18 prior to incubation and 73 ± 17 after incubation). As for the UV-VIS absorbance, AM did not present any substantial change whereas incubated BNC showed a small rise in absorbance at 600 nm compared to untreated BNC (from 0.38 to 0.41) (Fig. 4A). The material's superficial mass was also characterized after the corneal medium incubation test (Fig. 4B). BNC samples reduced its superficial mass near 12% (from 90 to 79 mg cm^{-2}) while AM samples decreased 33% its superficial mass (from 12 to 8 mg cm^{-2}). This change of the superficial mass was statistically significant (paired T-test, p-value < 0.0001) only for the AM specimens.

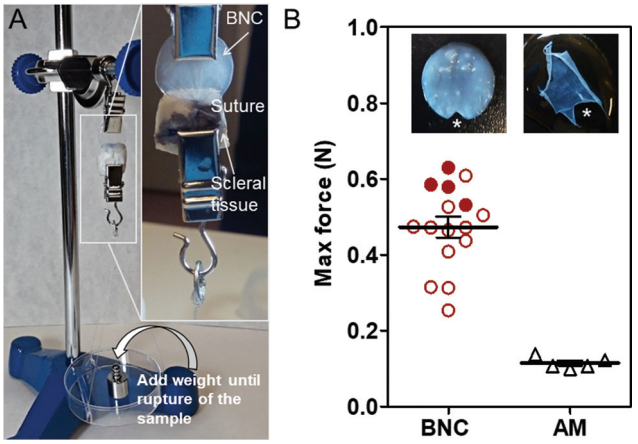

Fig. 2 Suture stress resistance test. (A) Set up of the device for the suture stress resistance test. The insert image shows a BNC sample sutured to a piece of scleral tissue. Same procedure was employed to evaluate AM. (B) Force (N) that caused the breakage of the materials. Filled circles indicate that BNC tolerated a higher weight than the suture thread. That is to say, the complex collapsed because the suture broke before the BNC. P-Value (unpaired T-test): <0.0001. Max forces were normalized for the maximum thickness sample of each group (986 μm for BNC and 63 μm for AM). Images inside the graph show the fracture of the material (indicated with asterisk) at the suture point.

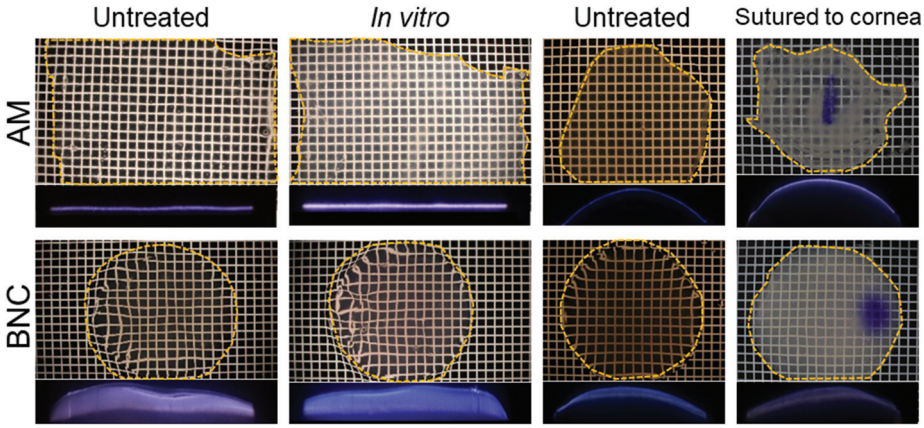

Fig. 3 Frontal (white filed + grid) and slit lamp images of AM and BNC before and after the stability tests. White field photographs were taken with a grid to better visualize transparency of the materials. Each square of the grid is one mm^2. Inserts at the bottom of the images correspond to lateral views of the materials captured with a slit lamp. In general, both materials were stable under the tested conditions and incubation times. To mark the orientation of the samples that were sutured to porcine corneas, a tissue marker was used. For clarity in the pictures, corneal bandages were delineated with a yellow-dotted-line.

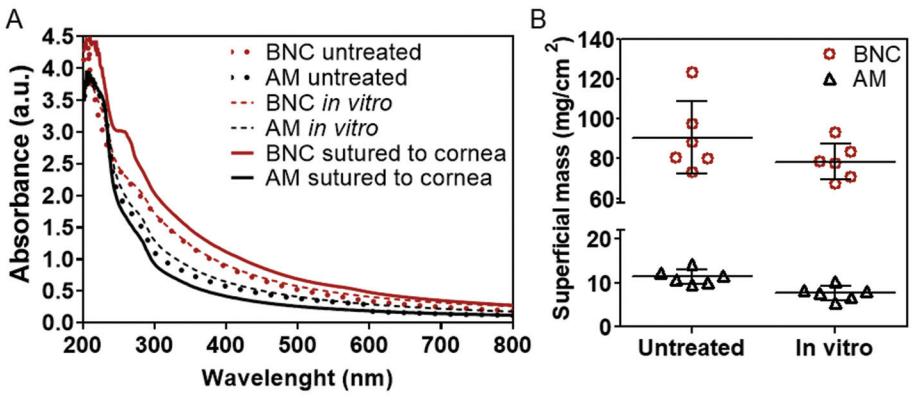

Fig. 4 Ultra violet-visible light absorbance of the materials and superficial mass. (A) Ultraviolet and visible light absorbance of BNC and AM materials at different experimental conditions. Average spectra were obtained from the mean of all the samples for each condition. As for samples sutured to porcine corneas, BNC increased its overall absorbance indicating some acquisition of the tissue/medium components. Oppositely, AM slightly decreases its absorbance, this might be due to a thinning of the material. (B) Changes in the superficial mass of the films upon 30-day maintenance *in vitro*. Superficial mass was compared to evaluate degradation and possible changes in thickness. Both materials experienced a reduction on its superficial mass: 12% for BNC and 33% for AM. This change in superficial mass was only statistically significant for AM (P-value < 0.0001, paired T-test) samples.

Finally, SEM investigation revealed that the characteristic nanofibrillar structure of both BNC and AM was retained during the 30-day experiment (Fig. 5, see untreated *vs. in vitro*) and that the epithelial side of AM presented some crystallizations after the *in vitro* incubation (ESI Fig. S3†). These elongated crystals, were undetectable by X-ray diffraction (data not shown) indicating that its contribution to the total amount of mass of the material should be rather small.

Conformability and adaptability of the materials to the arched shape of the cornea were evaluated by suturing BNC to porcine eyes. BNC films naturally present a flat side (with compact fibres) and a rougher side (loose fibres). After assessing the two possible orientations, the flat side was selected to be in contact with the corneal surface since it showed better adaptability. Importantly, corneal surgeons from our clinic sutured BNC to the cornea of over a score of excised pig eyes and found it easy to handle. BNC maintained its original shape during the process without tearing at the puncture holes. Overall, the suturing of BNC was comparable to that of AM and the sutured BNC molded well to the dome-shaped cornea. See ESI Fig. S4† for more details about this process.

Excised porcine corneas were also used for a more realistic *ex vivo* evaluation of the materials under study. Sample preparation for BNC is illustrated in Fig. 6 and AM samples were arranged in a similar fashion. After the *ex vivo* culture, the materials were recovered for characterization. Overall, we did

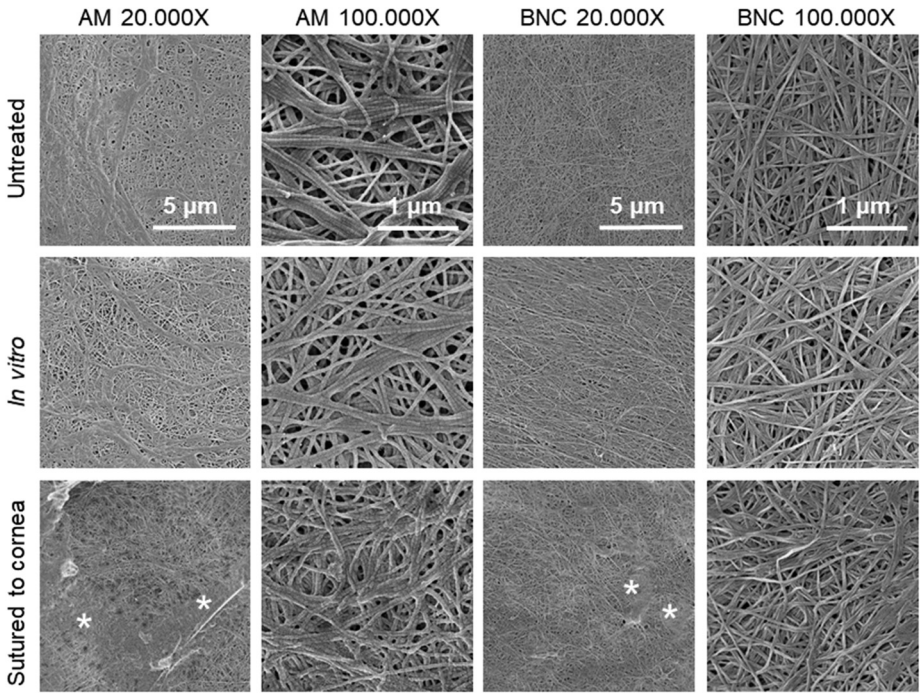

Fig. 5 Representative SEM images of the corneal bandage materials before and after the *in vitro* and *ex vivo* stability tests. The side of the material shown here is the one that was in contact with the eye surface, images from the external side are shown as ESI Fig. S3.† Under SEM, no signs of degradation were observed neither for BNC nor for AM samples after any of the two treatments. For the materials sutured to the corneas, both AM and BNC showed some organic deposits (marked with *) that might indicate some transfer of biological matter from the eye surface/culture medium to the ocular surface bandages.

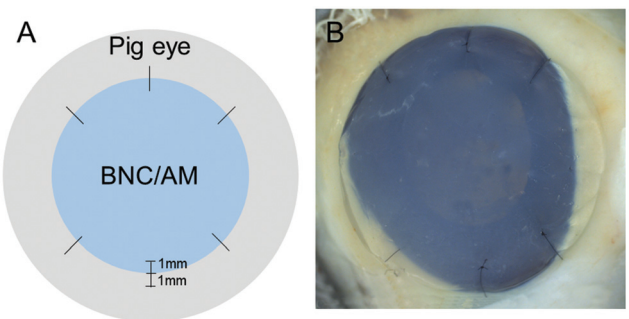

Fig. 6 *Ex vivo* suture test sample preparation. BNC hydrogels and AM were sutured to pig eyes as illustrated schematically in (A). The needle easily penetrated the BNC hydrogels and conventional knots were made with surgical instrumentation (B). Both materials adapted well to the dome shape of the eye without forming wrinkles. Then, the cornea and part of the sclera were excised and placed on Petri dishes containing RPMI medium for 20 days. Same sample preparation process was followed for AM.

not detect major differences in the BNC samples before and after being sutured to the excised porcine corneas; all samples maintained their integrity (size and shape) and did not degrade (for better visualization refer to dark field images in ESI Fig. S2†). AM samples also maintained their overall integrity but presented tears at the suture points and some debilitated (*i.e.* more transparent and apparently fragile) areas. Lateral images of the samples taken with a slit lamp showed a continuous layer of material both for AM and BNC after being sutured to the corneas (see third and fourth columns in Fig. 3) without detectable defects. Accordingly, SEM imaging revealed that the nanofibrillar structure of BNC and AM was maintained after their incubation (Fig. 5, see untreated *vs.* sutured to cornea) in contact with the biological material. Both BNC and AM presented some organic deposits on the side in contact with the corneal surface (indicated with asterisks in Fig. 5). The crystals that appeared on the *in vitro* experiment were not detected in these *ex vivo* conditions.

In comparison to untreated samples, BNC increased 26% its absorbance at 600 nm whereas AM samples displayed a reduction of 35% (see Fig. 4A). Moreover, BNC samples presented a new absorbance peak at 260 nm. It was not possible to accurately calculate the superficial mass of the samples after the *ex vivo* test since the suture caused deformation of the samples, especially of the AM membranes.

Discussion

Although BNC possesses attractive intrinsic characteristics to become a new ocular surface bandage material,[18,36] very few studies have explored this possibility. Here, we present a comparative study between BNC and the most common ocular surface bandage; AM. First, we provide an extensive character-

ization of BNC and AM and a comparison of their physicochemical characteristics. Then, BNC is positively evaluated regarding: stability under simulated physiological conditions, resistance to the mechanical stress caused by suture, conformability to the eye surface and easiness of manipulation using standard clinical procedures. Compared to AM, BNC hydrogels resisted a higher force on the suture stress test, did not lose transparency after the *in vitro* test and where less deformed on the *ex vivo* assay.

The present study focused on the suitability of BNC as a new ocular surface bandage from a material point of view. Therefore, data regarding the ability of BNC to promote corneal wound healing is not provided yet. We speculate that BNC corneal bandages can have a protective effect similar to that of collagen corneal shields.[37,38] Thus, feasible clinical usages of BNC would be as temporary tectonic or multi-layered bandages for patients suffering from non-infectious corneal ulcers, or ulcerative keratitis with high risk of corneal perforation. Applying a therapeutic contact lens on top of the BNC bandage could be needed, in the same way as when using AM in clinical practice. The contact lens would contribute to decrease friction with the inner surface of the eyelids as well as to maintain moisture by capturing the tears on its concave side.

Importantly, our latest data[39] shows that the amount of endotoxins detected in the eluates of autoclaved BNC are 0.05 ± 0.01 Endotoxin Units (EU) mL^{-1}. This value falls well below the Food and Drug Administration limit set at 0.5 EU mL^{-1} for medical devices and indicates that BNC can be considered a non-pyrogenic material. Regarding inflammatory responses, we expect native BNC to act as an inert biomaterial. That is, BNC hydrogels are expect to be neither pro nor anti-inflammatory as demonstrated in ref. 40 with *in vitro* tests. It has also been argued that BNC is well tolerated *in vivo* without causing major inflammatory complications.[41,42] However, the interactions of BNC with the immune system will be addressed on our future investigations.

BNC is a mechanical and thermally stable material. These features are relevant for thermal sterilization (typically performed at 121 °C) and for adhering BNC to the ocular surface by suture stitches. AM decomposition takes place at rather high temperatures but its sterilization by heat might compromise its wound healing capabilities. BNC hydrogels used in this study were much thicker than AM, although the thickness of both materials varies considerable due to its biological origin.[43,44] AM can be up to 200 μm and can be used as a multilayer, an approach that can also be envisioned for BNC. Notably, BNC's thickness can be modulated during the production process[45] and/or posteriorly by adjusting its water content[33] to meet specific requirements. Roughly, BNC hydrogels can be obtained with thicknesses ranging from hundreds of microns to few millimetres while dry BNC membranes exhibit thicknesses of tens of microns.

The Young modulus of BNC is also largely influenced by the water content and biosynthesis method, being in the range of 0.6 to 1.5 GPa [33,46] in its dry state with considerably lower values for the never dry form. Similarly, tensile strength is in the order of 50 MPa for dry BNC and between 1.5 and 2 MPa for the never dry form. Nevertheless, the BNC hydrogels present higher ductility with elongation at break values up to 20% which might be of interest for the application suggested here.[47] BNC presents a characteristic nanofibrillar structure with a great architectonical similarity to that of collagen found in the stromal side of AM (see SEM images in Fig. 1). Despite the observed similar nanofibrillar organization, BNC and AM differ at the organization level, evidenced by the X-ray diffraction patterns, being AM non-crystalline and BNC a semi-crystalline material.

On the other hand, BNC's nanofibrillar network can act as a reservoir for diverse molecules.[48,49] This capability might offer venues for future BNC corneal bandages supplemented with therapeutic agents in order to emulate the anti-scarring and anti-inflammatory effects that AM provides. In fact, the anti-inflammatory effect BNC hydrogels supplemented with diclofenac has recently been reported.[40] Similarly, in cases of bacterial keratitis, BNC could be impregnated with antibiotics to act as a medication reservoir. In this direction, BNC is also well known to support the culture of several cell types[50–52] including retinal pigment epithelial cells.[20,53] These reports, together with the findings presented here, suggest further uses of BNC as a cell carrier for corneal cell therapies. In the case of a BNC bandage supplemented with sensitive biological material (cells or bioactive molecules), the cryo-storage approach commonly used for preserving AM[54] could also be considered since our recent data demonstrate that BNC is stable at liquid nitrogen temperatures.[39] Other interesting modifications of BNC aim at increasing its optical transparency. This can be achieved by mechanically increasing fibre alignment[46] or by filling the pores with biocompatible polymers such as polyethylene glycol.[40]

Importantly, we validate that BNC can be sutured to the ocular surface without employing more time or resources than AM while presenting a higher resistance to the mechanical stress caused by the suture. Moreover, its soft and flexible nature confers optimal adaptability to the dome shape of the ocular surface. We also expect that the high liquid holding capacity of BNC hydrogels will be convenient to keep proper hydration of the ocular surface.

We examined the behaviour of BNC in two simulated physiological environments; *in vitro*, maintained in corneal preservation medium for 30 days, and *ex vivo*, sutured to excised pig corneas during 20 days without observing signs of degradation neither at the macro nor at the micro/nano scales. *In vitro*, BNC and AM kept its integrity but decreased its superficial mass; this reduction was higher in weight percentage for AM than for BNC. However, it is hard to discern if this shrinking in the superficial mass is due to material deterioration or to loss of water due to osmotic processes. Additionally, AM samples became more opaque after the incubation, possibly due to microcrystals deposits that increased light scattering. BNC hydrogels did not present crystals or opacification but BNC films were coloured by the culture medium and this

might be responsible of the slight increase of light absorbance.

Placing the materials in direct contact with ocular tissue on the *ex vivo* test allowed us to discard degradation of the BNC caused by the interaction with the tissue and to confirm its robustness after suturing. BNC nanofibrillar structure was also intact after the experiment. Contrary to BNC, AM samples were deformed and presented some tears at the suture points but kept its overall integrity. The UV-VIS light absorbance of AM was decreased after the treatment and some areas seemed to debilitate as observed on the grid images. This might be attributed to a thinning of the material that needs to be further confirmed. BNC behaved differently, its overall UV-VIS absorbance moderately increased presenting a new peak characteristic of nucleic acids and close to the protein absorbance region. This could be ascribed to the adsorption of biological material on the BNC coming either from the ocular tissues or the culture medium. This observation is also supported by the organic deposits visualized under SEM. Transference of tissue/medium components was also detected visually in the form of opaque areas and with SEM as organic accumulations in the AM samples. Overall, we consider BNC to be stable under the two tested conditions and times.

In summary, corneal damage is a highly prevalent cause of vision reduction and blindness, particularly in rural areas of developing countries. Therefore, there is an evident need for low-cost, accessible, durable and easy to apply ocular surface bandages.[55,56] In the present study, we aimed to elucidate whether BNC, a biomaterial that shows great promise for skin regeneration, is also suitable as bandage material to treat ocular surface disorders. Using AM as a benchmark, we demonstrated that BNC meets basic preclinical requirements for this purpose. These findings, together with BNC's prolonged shelf life, straightforward and animal-free production and controllability might encourage further investigations of BNC for corneal regeneration.

Methods

The general experimental design of this study is summarized on ESI Table 1.†

Amniotic membrane

Human AM were obtained from the local tissue bank (Barcelona Banc de Sang i Teixits) and stored at −80 °C until experimental use. The samples were cut into the desired shapes and sizes using a 17 mm ∅ trephine (circles) or surgical scissors (rectangles).

Production of the bacterial nanocellulose films

Bacterial nanocellulose films were obtained following our established protocol detailed elsewhere.[57] Briefly, a commercial *Komagataeibacter xylinus (K. xylinus)* strain (NCIMB 5346 from CECT, Valencia, Spain) was inoculated on 6 mL of Hestrin–Schramm (HS) medium (1.15 g citric acid, 6.8 g $Na_2HPO_4{\cdot}12H_2O$, 5 g peptone, 5 g yeast, and 20 g dextrose for 1 L of Milli-Q water) and incubated statically for 7 days at 30 °C. This bacterial culture was further diluted 1 : 15 with fresh HS medium and cultured on 24-well plates (2 mL per well) during 3 days. The BNC pellicles that formed at the air–liquid interface were collected and immersed in a solution of 1 : 1 ethanol : deionized water (DI) to kill the bacteria. Then, the films were washed 1 × 40 minutes in boiling DI water and 2 × 20 minutes in a boiling 0.1 M NaOH solution to remove organic residues. After rinsing several times with DI water, the films were autoclaved (121 °C, 20 min).

Endotoxin contamination study

The endotoxin extraction was carried out by placing clean and autoclaved BNC hydrogels in depyrogenated falcon tubes with 40 mL of endotoxin free water during 72 h at 30 °C and under orbital agitation (100 rpm), according to FDA recommendations.[58] The endotoxin content in the eluates from BNC samples was measured with a Pierce™ LAL Chromogenic Endotoxin Quantification Kit purchased form Thermo Fisher and the assay was performed following the manufacture's instructions. The products of the reaction were read for absorbance at 405 nm in a microplate reader (Infinite 200 PRO, TECAN®) at 37 °C. The indicated values in the results section correspond to mean ± standard deviation of two independent experiments obtained from two different endotoxin quantification kits and evaluating each time two samples from two different batches of BNC.

Dehydration test

Three independent BNC hydrogels (12 cm × 12 cm) were left to dehydrate inside a room with controlled humidity (45%) and temperature (22 °C). The materials were weighed every hour with a precision scale. The initial weight of the hydrogels was used to calculate the reaming weight (%) at different time points.

Thickness measurements

Thickness of the AM (n = 12) and BNC (n = 20) samples was measured with a digital micrometre, placing the samples between two cover slides to keep them flat. A slight blotting of the specimens was made with filter paper prior to the measurement to remove the excess of liquid. Five measures were made for each sample at different areas to get an average thickness.

Thermogravimetric analysis

To evaluate the thermal stability of the materials, a TGA-DSC/DTA analyser (NETZSCH STA 449 F1 Jupiter) was used. The covered temperature range was from 25 to 800 °C and the heating rate was 10 °C per minute in air. The first derivative graphs were obtained with the Origin 85 software. Three samples were analysed from each material.

X-Ray diffraction

Dry BNC and AM were fixed flat on a silicon wafer support to acquire X-ray diffraction patterns using a Siemens (Model D-5000) diffractometer. Step size was 0.02° per minute in a 2θ range from 5° to 30°. A Cu anode was employed. Smoothing of the data was performed with the Savitzky–Golay model included on the Origin 85 software.

Digital images

Digital images were taken with a Canon Eos 550C camera coupled to a microscope with the samples placed on a dark/white field chamber. For the white field images, a grid (squares of 1 mm^2) was located under the specimens to better visualize transparency of the materials. The photographs were acquired with a standardized exposure time of 1/100 s. Areas and grey values were measured from these images with the ImageJ-win64 software.

Scanning electron microscopy

Both BNC and AM samples were freeze dried at −80 °C for 48 hours to preserve its native structure. Small pieces of the films were cut with scissors and immobilized on top of aluminium sample holder with a carbon tape. The samples were sputtered with 5 nm of platinum before being imaged with a high resolution scanning electron microscope Magellan 400L at the following magnifications: 5000X, 20 000X and 100 000X. The employed voltage was 2.00 kV and the current was 100 pA.

Ultraviolet visible spectroscopy

Ultraviolet-visible (UV-Vis) absorbance spectra of BNC and AM materials were obtained without any sample preparation step. A Varian Cary-5000 UV-Vis-NIR spectrophotometer on transmission mode was employed to obtain a minimum of two spectra (between 200 and 800 nm) from each sample. A baseline correction was performed by subtracting the absorbance of the glass coverslips used to hold the samples. The absorbance of the sample was calculated as: $A = \log_{10}(I_0/I)$ where I_0 corresponds to the intensity of the light passing through the reference cell (glass) and I to the intensity of the light passing through the sample cell (BNC or AM) at the same wavelength.

In vitro stability test

The *in vitro* stability test evaluated six independent samples of each material. Circular BNC films of ≈2 cm^2 and AM rectangles of ≈3 cm^2 were used. Every sample was weighed and photographed before the incubation. Each sample was placed individually on sterile glass bottles containing 100 mL of Tissue C (Alchimia) culture medium. The materials were clipped to a CornealFloat to keep them suspended in the liquid. The bottles were kept during 30 days in a CO_2 incubator (5%) at 37 °C. Then, the materials were recovered and characterized for: weight, diameter, integrity, micro/nano structure (SEM) and light absorbance (UV-Vis).

Suture stretch test

To test the mechanical stability of the materials, the device illustrated in Fig. 2A was employed. BNC (n = 16) and AM (n = 5) samples were sutured (Suture type: Nylon 10/0, Lab Aragó) with a single stitch to small pieces of porcine scleral tissue (≈1 cm^2) using standard suture instruments from Grieshaber (Westcott scissors and Colibrí forceps), a Barraquer needle holder and a Castroviejo Suture forceps. Then, the complex was clamped on the top part (clamp placed on the BNC/AM) and fixed to a support. Another clamp was placed at the scleral tissue (bottom) and a platform was hung form that clamp. 4.5 g weights were added gradually (every two minutes) to the platform until the BNC/AM broke at the suture point. The maximum weight tolerated by each sample before rupture was divided by the normalized thickness of the sample inside each type (BNC and AM). A value of 1 was assigned to the thickest BNC (986 μm) and AM (63 μm) specimens.

Ex vivo suture test

Eyes globes were obtained from 6 month old pigs and used within 48 h. BNC and AM films of ≈16 mm diameter were non-invasively characterized (weight and diameter) and then sutured to pig corneas keeping the limbal area intact. 6 symmetric sutures were made for each eye 1 mm away from the BNC/AM border and holding 1 mm of tissue with standard nylon suture 10/0 from Lab Aragó (Barcelona). The knots were not buried. The sutures penetrated $\approx\frac{3}{4}$ of the cornea/sclera thickness. The cornea and part of the sclera were resected from the rest of the eye with scleral scissors. Pictures were also taken at this point. The samples were decontaminated by immersion into a 5% Povidone–iodine (PI) solution during 2 minutes. Sodium thiosulphate (0.1%) was used to remove the PI and later the samples were rinsed with phosphate-buffered saline. Then, the excised corneas were placed in a closed container (Petri dish) with 13 mL of Roswell Park Memorial Institute (RPMI-1640) culture medium (R8758 Sigma-Aldrich) supplemented with 5% fetal bovine serum (F7524 Sigma-Aldrich) and 1% antibiotic–antimycotic (A5955 Sigma-Aldrich) under sterile conditions. The as-prepared Petri dishes were kept in an incubator at 37 °C and 5% CO_2 for 20 days. Medium was changed every 3 to 4 days.

Statistical analysis

For the statistical analysis, GraphPad Prism 5 software was employed. Data is represented by mean ± standard deviation. Statistical significance was accepted when p-values under 0.05 were obtained in paired (superficial mass) or unpaired (suture stress test) Student's T-tests.

Author contributions

I.A.S designed experiments, prepared and cultured samples, characterized the samples, acquired data, analysed data, interpreted data, prepared the figures, wrote the manuscript, revised the manuscript; J.C.D designed experiments, prepared

and cultured samples, acquired data, interpreted data, revised the manuscript; J. F. E. performed the sutures; provided clinical advice and revised the manuscript; V.C. provided literature, revised experiments, revised the manuscript A. L., A. R. and R. M. designed and supervised experiments, interpreted data, revised the manuscript and obtained funding.

Data availability

The data generated during and/or analysed during the current study are available from the corresponding author on reasonable request.

Conflicts of interest

The author(s) declare no competing interests.

Acknowledgements

Authors acknowledge financial support from the Spanish Ministry of Science and Innovation through the RTI2018-096273-B-I00, project, the 'Severo Ochoa' Programme for Centers of Excellence in R&D (SEV-2015-0496) and the PhD scholarship of I. A. S. (BE-2017-076734) and the Generalitat de Catalunya with the 2017SGR765 and the 2019LLAV00046 projects. Authors also thank María Jesús Sánchez-Guisadofor for her assistance with the endotoxin study. The ICMAB technical services (TGA and X-Ray) and Marcos Rosado from the ICN2 electron microscopy service are acknowledged. The ICMAB members (IAS, AL, AR) participate in the CSIC Interdisciplinary Platform for Sustainable Plastics towards a Circular Economy, SUSPLAST and in the Aerogels COST ACTION (CA 18125). We acknowledge support of the publication fee by the CSIC Open Access Publication Support Initiative through its Unit of Information Resources for Research (URICI).

References

1 M. J. Burton, Corneal blindness: Prevention, treatment and rehabilitation, *Community Eye Health*, 2009, **22**, 33–35.
2 J. P. Whitcher, M. Srinivasan and M. P. Upadhyay, *Corneal blindness: a global perspective*, 2001.
3 T. P. H. Gundersen, Conjunctival flaps for corneal disease: their usefulness and complications, *Trans. Am. Ophthalmol. Soc.*, 1969, **67**, 78–95.
4 J. J. Arentsen, P. R. Laibson and E. J. Cohen, Management of corneal descemetoceles and perforations, *Trans. Am. Ophthalmol. Soc.*, 1984, **82**, 92–105.
5 A. M. Alino, H. D. Perry, A. J. Kanellopoulos, E. D. Donnenfeld and E. K. Rahn, Conjunctival flaps, *Ophthalmology*, 1998, **105**, 1120–1123.
6 C. Y. Su and C. P. Lin, Combined use of an amniotic membrane and tissue adhesive in treating corneal perforation: a case report, *Ophthalmic Surg. Lasers*, 2000, **31**, 151–154.
7 H.-J. Chen, R. T. Pires and S. C. Tseng, Amniotic membrane transplantation for severe neurotrophic corneal ulcers, *Br. J. Ophthalmol.*, 2000, **84**, 826–833.
8 E. H. Yildiz, *et al.*, Amniotic Membrane Transplantation: Indications and Results, *Eur. J. Ophthalmol.*, 2008, **18**, 685–690.
9 D. Meller, *et al.*, Amniotic membrane transplantation for acute chemical or thermal burns, *Ophthalmology*, 2000, **107**, 980–989.
10 G. Bourne, THE FOETAL MEMBRANES A Review of the Anatomy of Normal Amnion and Chorion and Some Aspects of Their Function, *Postgrad. Med.*, 1962, **38**, 193–201.
11 A. Solomon, *et al.*, Amniotic membrane grafts for nontraumatic corneal perforations, descemetoceles, and deep ulcers, *Ophthalmology*, 2002, **109**, 694–703.
12 A. Paolin, *et al.*, Amniotic membranes in ophthalmology: long term data on transplantation outcomes, *Cell Tissue Banking*, 2016, **17**, 51–58.
13 M. Kaup, C. Redbrake, N. Plange, K. Arend and A. Remky, Amniotic membrane transplantation in severe ocular surface disorders, *Eur. J. Ophthalmol.*, 2008, **18**, 691–694.
14 C. C. de Farias, N. Allemann and J.ÁP. Gomes, Randomized Trial Comparing Amniotic Membrane Transplantation with Lamellar Corneal Graft for the Treatment of Corneal Thinning, *Cornea*, 2016, **35**, 438–444.
15 S. Majumdar, *et al.*, Cyclodextrin Modulated Type I Collagen Self-Assembly to Engineer Biomimetic Cornea Implants, *Adv. Funct. Mater.*, 2018, **28**, 1804076.
16 A. Sorkio, *et al.*, Human stem cell based corneal tissue mimicking structures using laser-assisted 3D bioprinting and functional bioinks, *Biomaterials*, 2018, **171**, 57–71.
17 L. Koivusalo, *et al.*, Tissue adhesive hyaluronic acid hydrogels for sutureless stem cell delivery and regeneration of corneal epithelium and stroma, *Biomaterials*, 2019, **225**, 119516.
18 H. Ullah, F. Wahid, H. A. Santos and T. Khan, Advances in biomedical and pharmaceutical applications of functional bacterial cellulose-based nanocomposites, *Carbohydr. Polym.*, 2016, **150**, 330–352.
19 H. G. de Oliveira Barud, *et al.*, A multipurpose natural and renewable polymer in medical applications: Bacterial cellulose, *Carbohydr. Polym.*, 2016, **153**, 406–420.
20 S. Gonçalves, *et al.*, Bacterial Cellulose As a Support for the Growth of Retinal Pigment Epithelium, *Biomacromolecules*, 2015, **16**, 1341–1351.
21 W. Czaja, A. Krystynowicz, S. Bielecki and R. M. Brown, Microbial cellulose - The natural power to heal wounds, *Biomaterials*, 2006, **27**, 145–151.
22 M. H. Kwak, *et al.*, Bacterial cellulose membrane produced by Acetobacter sp. A10 for burn wound dressing applications, *Carbohydr. Polym.*, 2015, **122**, 387–398.
23 Y. Li, *et al.*, Evaluation of the Effect of the Structure of Bacterial Cellulose on Full Thickness Skin Wound Repair on a Microfluidic Chip, *Biomacromolecules*, 2015, **16**, 780–789.

24 F. Robotti, *et al.*, Microengineered biosynthesized cellulose as anti-fibrotic in vivo protection for cardiac implantable electronic devices, *Biomaterials*, 2020, **229**, 119583.
25 C. Fey, *et al.*, Bacterial nanocellulose as novel carrier for intestinal epithelial cells in drug delivery studies, *Mater. Sci. Eng., C*, 2020, **109**, 110613.
26 P. Weyell, *et al.*, Tailor-made material characteristics of bacterial cellulose for drug delivery applications in dentistry, *Carbohydr. Polym.*, 2019, **207**, 1–10.
27 L. Bacakova, *et al.*, Versatile Application of Nanocellulose: From Industry to Skin Tissue Engineering and Wound Healing, *Nanomaterials*, 2019, **9**, 164.
28 F. d. M. T. Lima, F. C. M. Pinto, B. L. d. S. Andrade-da-Costa, *et al.*, Biocompatible bacterial cellulose membrane in dural defect repair of rat, *J. Mater. Sci.: Mater. Med.*, 2017, **28**, 37.
29 I. Anton-Sales, U. Beekmann, A. Laromaine, A. Roig and D. Kralisch, Opportunities of Bacterial Cellulose to Treat Epithelial Tissues, *Curr. Drug Targets*, 2018, **20**, 808–822.
30 A. Laromaine, *et al.*, Free-standing three-dimensional hollow bacterial cellulose structures with controlled geometry *via* patterned superhydrophobic–hydrophilic surfaces, *Soft Matter*, 2018, **14**, 3955–3962.
31 D. Abol-Fotouh, *et al.*, Farming thermoelectric paper, *Energy Environ. Sci.*, 2019, **12**, 716–726.
32 A. Azuara-Blanco and D. H. Pillai CT, Amniotic membrane transplantation for ocular surface reconstruction, *Br. J. Ophthalmol.*, 1999, **83**, 399–402.
33 M. Zeng, A. Laromaine and A. Roig, Bacterial cellulose films: influence of bacterial strain and drying route on film properties, *Cellulose*, 2014, **21**, 4455–4469.
34 Y. Pei, *et al.*, Effectively promoting wound healing with cellulose/gelatin sponges constructed directly from a cellulose solution, *J. Mater. Chem. B*, 2015, **3**, 7518–7528.
35 F. Küng, D. W. Schubert, P. Stafiej, F. E. Kruse and T. A. Fuchsluger, A novel suture retention test for scaffold strength characterization in ophthalmology, *Mater. Sci. Eng., C*, 2016, **69**, 941–946.
36 M. Jorfi and E. J. Foster, Recent advances in nanocellulose for biomedical applications, *J. Appl. Polym. Sci.*, 2015, **132**, 1–19.
37 J. V. Aquavella, M. del Cerro, P. S. Musco, S. Ueda and M. D. DePaolis, The effect of a collagen bandage lens on corneal wound healing: a preliminary report, *Ophthalmic Surg.*, 1987, **18**, 570–573.
38 C. E. Willoughby, M. Batterbury and S. B. Kaye, Collagen corneal shields, *Surv. Ophthalmol.*, 2002, **47**, 174–182.
39 I. Anton-Sales, S. Roig-Sánchez, M.-J. Sánchez-Guisado, A. Laromaine and A. Roig, *Bacterial Nanocellulose and Titania Hybrids: Cytocompatible and Cryopreservable Cell Carriers*, 2020, submitted.
40 U. Beekmann, *et al.*, Process control and scale-up of modified bacterial cellulose production for tailor-made anti-inflammatory drug delivery systems, *Carbohydr. Polym.*, 2020, **236**, 116062.
41 M. Osorio, *et al.*, Ex Vivo and In Vivo Biocompatibility Assessment (Blood and Tissue) of Three-Dimensional Bacterial Nanocellulose Biomaterials for Soft Tissue Implants, *Sci. Rep.*, 2019, **9**, 10553.
42 H. Martínez Ávila, *et al.*, Novel bilayer bacterial nanocellulose scaffold supports neocartilage formation in vitro and in vivo, *Biomaterials*, 2015, **44**, 122–133.
43 A. F. S. Costa, F. C. G. Almeida, G. M. Vinhas and L. A. Sarubbo, Production of Bacterial Cellulose by Gluconacetobacter hansenii Using Corn Steep Liquor As Nutrient Sources, *Front. Microbiol.*, 2017, **8**, 2027.
44 A. McGaughy, *et al.*, In Office Use of Amniotic Membrane, *Cornea*, 2015, 31–32.
45 W. Borzani and S. J. de Souza, Mechanism of the film thickness increasing during the bacterial production of cellulose on non-agitaded liquid media, *Biotechnol. Lett.*, 1995, **17**, 1271–1272.
46 S. Wang, *et al.*, Transparent, Anisotropic Biofilm with Aligned Bacterial Cellulose Nanofibers, *Adv. Funct. Mater.*, 2018, **28**, 1707491.
47 Own data, not published.
48 S. Moritz, *et al.*, Active wound dressings based on bacterial nanocellulose as drug delivery system for octenidine, *Int. J. Pharm.*, 2014, **471**, 45–55.
49 G. F. Picheth, *et al.*, Lysozyme-triggered epidermal growth factor release from bacterial cellulose membranes controlled by smart nanostructured films, *J. Pharm. Sci.*, 2014, **103**, 3958–3965.
50 T. Tronser, A. Laromaine, A. Roig and P. A. Levkin, Bacterial Cellulose Promotes Long-Term Stemness of mESC, *ACS Appl. Mater. Interfaces*, 2018, **10**, 16260–16269.
51 S. Taokaew, M. Phisalaphong and B.-M. Z. Newby, Modification of Bacterial Cellulose with Organosilanes to Improve Attachment and Spreading of Human Fibroblasts, *Cellulose*, 2015, **22**, 2311–2324.
52 A. Bodin, *et al.*, Tissue-engineered conduit using urine-derived stem cells seeded bacterial cellulose polymer in urinary reconstruction and diversion, *Biomaterials*, 2010, **31**, 8889–8901.
53 S. Gonçalves, *et al.*, Acetylated bacterial cellulose coated with urinary bladder matrix as a substrate for retinal pigment epithelium, *Colloids Surf., B*, 2016, **139**, 1–9.
54 K. Jirsova and G. L. A. Jones, Amniotic membrane in ophthalmology: properties, preparation, storage and indications for grafting—a review, *Cell Tissue Banking*, 2017, **18**, 193–204.
55 E. Shirzaei Sani, *et al.*, Sutureless repair of corneal injuries using naturally derived bioadhesive hydrogels, *Sci. Adv.*, 2019, **5**, 1281.
56 M. M. Islam, *et al.*, Biomaterials-enabled cornea regeneration in patients at high risk for rejection of donor tissue transplantation, *npj Regener. Med.*, 2018, **3**, DOI: 10.1038/s41536-017-0038-8.
57 S. Roig-Sanchez, *et al.*, Nanocellulose films with multiple functional nanoparticles in confined spatial distribution, *Nanoscale Horiz.*, 2019, **4**, 634–641.
58 U.S. Department of Health and Human Services, *et al. Guidance for Industry Pyrogen and Endotoxins Testing: Questions and Answers*, 2012.

